Article

Fabrication of Monodisperse Asymmetric Colloidal Clusters by Using Contact Area Lithography (CAL)

Changdeuck Bae, Jooho Moon, Hyunjung Shin, Jiyoung Kim, and Myung M. Sung

J. Am. Chem. Soc., **2007**, 129 (46), 14232-14239• DOI: 10.1021/ja073043p • Publication Date (Web): 27 October 2007

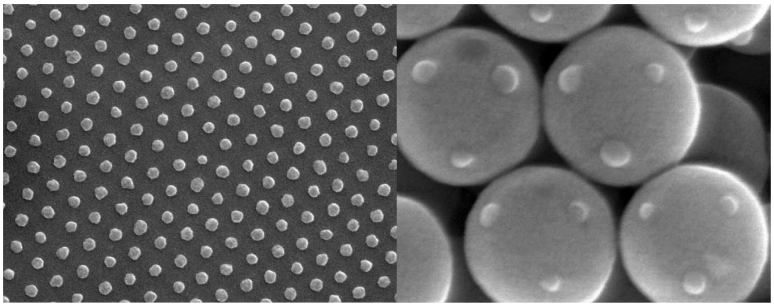

J|A|C|S
ARTICLES
Published on Web 10/27/2007

Fabrication of Monodisperse Asymmetric Colloidal Clusters by Using Contact Area Lithography (CAL)

Changdeuck Bae,[†] Jooho Moon,[‡] Hyunjung Shin,*[,†] Jiyoung Kim,[§] and Myung M. Sung[||]

Contribution from the Center for Materials and Processes of Self-Assembly and School of Advanced Materials Engineering, Kookmin University, Seoul 136-702, Korea, Department of Materials Science and Engineering, Yonsei University, Seoul 120-749, Korea, Department of Electrical Engineering, University of Texas, Dallas, Richardson, Texas 75080, and Department of Chemistry, Hanyang University, Seoul 133-791, Korea

Received May 1, 2007; E-mail: hjshin@kookmin.ac.kr

Abstract: We report a new fabrication method of asymmetric colloidal clusters by using contact area lithography with site-selective growth. Nanometric surface patterns (~44, 60, and 81 nm in diameter) were prepared by coating surfaces with self-assembled monolayers (SAMs; octadecyltrichlorosilane (OTS) in this study) except the contact area either between colloidal particles or between colloids and substrate. Nanoscale site-specific heterogeneous nucleation and growth of oxide materials of titanium were studied using the patterns of OTS-SAMs onto the either flat or curved surfaces of SiO_2. Experimental results suggest that a combination of the large difference in the surface energy between the growing and surrounding surfaces and the diffusion-controlled growth leads to complete nanoscale site specificity. We also fabricated superstructrures of silica spheres with hemispheres of titania (<20 nm in dimension) on their surfaces and discussed the optical properties of colloidal films consisting of the monodisperse asymmetric colloidal clusters in terms of photonic band gap.

1. Introduction

Dielectric materials arrayed periodically with appropriate spacings, widely known as "photonic crystals," exhibit different colors according to their glancing angles as caused by changes in the symmetry of the structure as it interacts with light in space.[1,2] Although the self-assembly of monodisperse spherical colloids has served as a facile route to create three-dimensional dielectric structures over the past two decade, results from theoretical studies testify that a close-packed face-centered-cubic (fcc) lattice for dielectric spheres does not possess a full band gap in which the propagation of light waves is forbidden for all wave vectors.[3] This is known to be due to the degeneracy at the *W* point of the first Brillouin zone that is induced by the symmetry of the fcc lattice. Yablonovitch and his colleagues have calculated and shown that employing nonspherical dielectric atoms can possibly break this degeneracy.[4] Two main types of nonspherical particles can be suggested for achieving the asymmetry (i.e., shape-anisotropic[5] and dielectrically anisotropic[6] particles). For shape-anisotropic particles, a variety of methods have been reported, for example, plastic deformation under high-energy ion irradiation,[7] mechanical stretching,[8] a swelling polymer and subsequent phase separation,[9] and a controlled sol−gel process.[10] However, fabricating dielectrically anisotropic colloids presents a significant challenge. Recent studies have been reported that dielectric colloidal clusters can be formed by attaching several colloidal particles on the surfaces of a colloidal sphere during solution processing in a random fashion.[11] Only a few cases of metallodielectric particles with regular geometry have been reported:[12] Monodisperse colloids with gold dots on their surfaces have been formed either by dewetting deposited gold half-shells or by evaporating gold

[†] Kookmin University.
[‡] Yonsei University.
[§] University of Texas.
[||] Hanyang University.

(1) Yablonovitch, E. *Phys. Rev. Lett.* **1987**, *58*, 2059.
(2) John, S. *Phys. Rev. Lett.* **1987**, *58*, 2486.
(3) (a) Ho, K. M.; Chan, C. T.; Soukoulis, C. M. *Phys. Rev. Lett.* **1990**, *65*, 3125. (b) Leung, K. M.; Liu, Y. F. *Phys. Rev. Lett.* **1990**, *65*, 2646.
(4) Yablonovitch, E.; Gmitter, T. J.; Leung, K. M. *Phys. Rev. Lett.* **1991**, *67*, 2295.
(5) (a) Haus, J. W.; Sözüer, H. S.; Inguva, R. *J. Mod. Opt.* **1992**, *32*, 1991. (b) Sözüer, H. S.; Haus, J. W.; Inguva, R. *Phys. Rev. B* **1992**, *45*, 13962.
(6) Li, Z. Y.; Wang, J.; Gu, B. Y. *Phys. Rev. B* **1998**, *58*, 3721.
(7) (a) Snoeks, E.; van Blaaderen, A.; van Dillen, T.; van Kats, C. M.; Brongersma, M. L.; Polman, A. *Adv. Mater.* **2000**, *12*, 1511. (b) van Dillen, T.; Polman, A.; Fukarek, W.; van Blaaderen, A. *Appl. Phys. Lett.* **2001**, *78*, 910. (c) Velikov, K. P.; van Dillen, T.; Polman, A.; van Blaaderen, A. *Appl. Phys. Lett.* **2001**, *81*, 838.
(8) (a) Lu, Y.; Yin, Y.; Xia, Y. *Adv. Mater.* **2001**, *13*, 271. (b) Arsenault, A. C.; Clark, T. J.; Freymann, G. V.; Cademartiri, L.; Sapienza, R.; Bertolotti, J.; Vekris, E.; Wong, S.; Kitaev, V.; Manners, I.; Wang, R. Z.; John, S.; Wiersma, D.; Ozin, G. A. *Nat. Mater.* **2006**, *5*, 179.
(9) (a) Skjeltorp, A. T.; Ugelstad, J.; Ellingsen, T. *J. Colloid Interface Sci.* **1996**, *113*, 577. (b) Okubo, M.; Yamashita, T.; Suzuki, T.; Shimizu, T. *Colloid Polym. Sci.* **1997**, *275*, 288. (c) Sheu, H. R.; El-Aasser, M. S.; Vanderhoff, J. W. *Polym. Mater. Sci. Eng.* **1988**, *59*, 1185.
(10) (a) Liddell, C. M.; Summers, C. J. *Adv. Mater.* **2003**, *15*, 1715. (b) Ibisate, M.; Zou, Z.; Xia, Y. *Adv. Funct. Mater.* **2006**, *16*, 1627.
(11) (a) Reculusa, S.; Mingotaud, C.; Bourgeat-Lami, E.; Duguet, E.; Ravaine, S. *Nano Lett.* **2004**, *4*, 1677. (b) Yi, G.-R.; Manoharan, V. N.; Michel, E.; Elsesser, M. T.; Yang, S.-M.; Pine, D. J. *Adv. Mater.* **2004**, *16*, 1204.
(12) (a) Zhang, G.; Wang, D.; Möhwald, H. *Nano Lett.* **2005**, *5*, 143. (b) Lu, Y.; Xiong, H.; Jiang, X.; Xia, Y.; Prentiss, M.; Whitesides, G. M. *J. Am. Chem. Soc.* **2003**, *125*, 12724.

10.1021/ja073043p CCC: $37.00

using ordered interstices in thin colloidal crystals as masks. In addition to these Au/silica and Au/polystyrene colloids, the monodisperse asymmetric ceramic colloidal clusters (e.g., titania/silica) with controlled geometry as well as mechanical stability should have potential for photonic and rheological applications.

Recently, we developed a patterning method, termed contact area lithography (CAL), that can easily create periodic surface patterns with high chemical contrasts (contact angle difference $\approx 110°$) at the sub-100 nm length scale by patterning the contact areas between a two-dimensional colloidal film and a substrate with self-assembled monolayers (SAMs).[13] Here we report a new fabrication method for preparing asymmetric colloidal clusters (ACCs) by combining CAL with nanoscale site-selective nucleation and growth on colloidal crystal surfaces. The surface nanopatterns prepared by CAL underwent a modified sol−gel process, resulting in site-selective deposition of titania only onto the opening (i.e., nucleation sites) of hydroxyl surfaces surrounded by octadecyltrichlorosilane (OTS)-SAMs. The growth behavior of titania on the chemical patterns was monitored as a function of both the deposition time and size of the oxide opening (~44, 60, and 81 nm in diameter). The results indicate that a significant difference in the surface energy between the growing and surrounding surfaces leads to a completely selective nucleation and growth and that the diffusion-controlled reaction process with appropriate precursors results in nanodots that are exceptionally uniform in size. It was also shown that this bottom-up approach can be applied to curved surfaces (i.e., the surfaces of colloidal particle with a diameter of 100 to 650 nm), producing ACCs as an example of assembling objects with nanometric decoration in a controlled manner. Furthermore, the optical properties of colloidal films consisting of these anisotropic particles were discussed as photonic band gap materials.

2. Experimental Section

Synthesis of Monodisperse Silica Colloids. Tetraethoxyl orthosilicate (TEOS, 99.999%, Aldrich), ethanol (anhydrous, Carlo Erba), and ammonia solution (28−30%, Junsei Chem., Japan) were from commercially available sources and were used without further purification. A mixture of 5 mL of TEOS and 30 mL of ethanol was injected into a mixture of 9.5 mL of NH_4OH and 60 mL of ethanol under vigorous magnetic stirring at a constant feeding rate using a syringe pump. The diameter of the silica beads was controlled by varying the feeding rate; this ranged from 0.1 to 50 mL·min^{-1}. After ~16 h, a white precipitate was harvested by centrifugation, followed by repetitively washing with ethanol and distilled water. This was then dried in a vacuum at 100 °C overnight.

Colloidal Crystallization. Monodisperse silica colloids were redispersed in ethanol in a vial. A piece (1×10 cm^2) of silicon wafer or a glass microscope slide was vertically submerged in the silica solution and then dried in an environmental chamber (R.H. = 74% and 45 °C) for approximately 10 days. The thickness of the silica colloidal films was adjusted by controlling the silica contents (typically 0.07−0.21 wt %).

Selective Deposition of Titania. In a typical synthesis, a mixture of 0.2 mL of titanium *tert*-butoxide (Aldrich) and 30 mL of ethylene glycol (Duksan, Korea) was magnetically stirred overnight and used as a precursor solution. Samples for either planar or curved growth were immersed in a mixture of 40 mL of acetone (anhydrous, Carlo Erba) and 0.1 mL of water. A 2 mL aliquot of precursor solution was immediately added to the acetonic medium and stirred gently. After the desired reaction time, the samples were taken out of the solution and washed with pure ethanol several times.

Scheme 1. Schematic Illustration of the Site-Selective Growth Process on Planar Substrates[a]

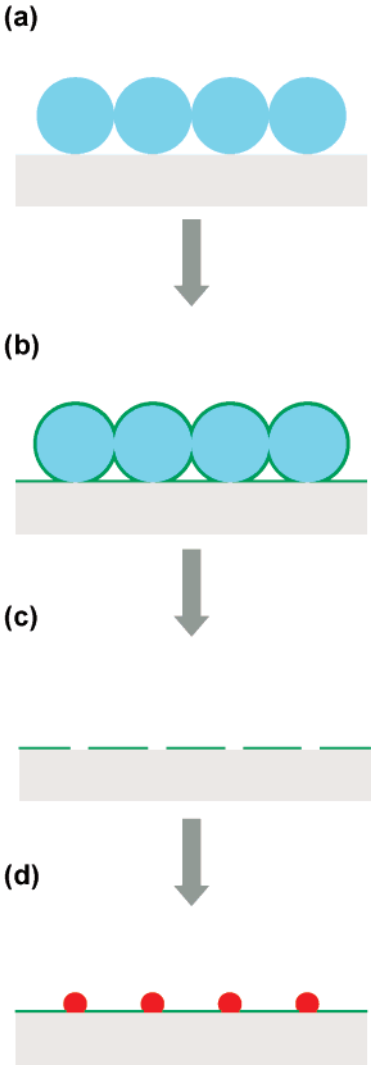

[a] (a) Sub-micrometer silica spheres are crystallized in two-dimension on SiO_2 substrates through convective assembly. (b) OTS molecules are self-assembled on the whole surfaces of silica except for the contact area between the 2D colloids and substrate in an OTS molecules-containing toluene solution. (c) The SAM-coated 2D colloids are detached by sonication in water. (d) The chemically nanopattered surfaces are served as templates for the site-specific nucleation and growth.

Electron Micrographs. The geometry and dimension of the resulting structures were investigated by field-emission scanning electron microscopy (FESEM, JSM7000F, JEOL, Japan) and high-resolution transmission electron microscopy (HRTEM, JEM2100F, JEOL, Japan). TEM samples were prepared by mechanically transferring the as-synthesized particles onto a substrate to a TEM grid. The map and spectroscopy by energy-dispersive X-ray spectrometry were recorded using an Oxford Inca Energy (Oxford Instruments, U.K.) equipped with JEM2100F.

Optical Characterization. To analyze the optical properties, titania/silica particles were prepared from thin colloidal crystals 465 and 650 nm silica in diameter on glass substrates by the proposed method. Optical absorption spectra were taken in the visible and NIR region from these samples with the incident light normal to the [111] surface of the sample (UV−vis spectrophotometer, UV-3150, Shimadzu, Japan).

(13) Bae, C.; Shin, H.; Moon, J.; Sung, M. M. *Chem. Mater*. **2006**, *18*, 1085.

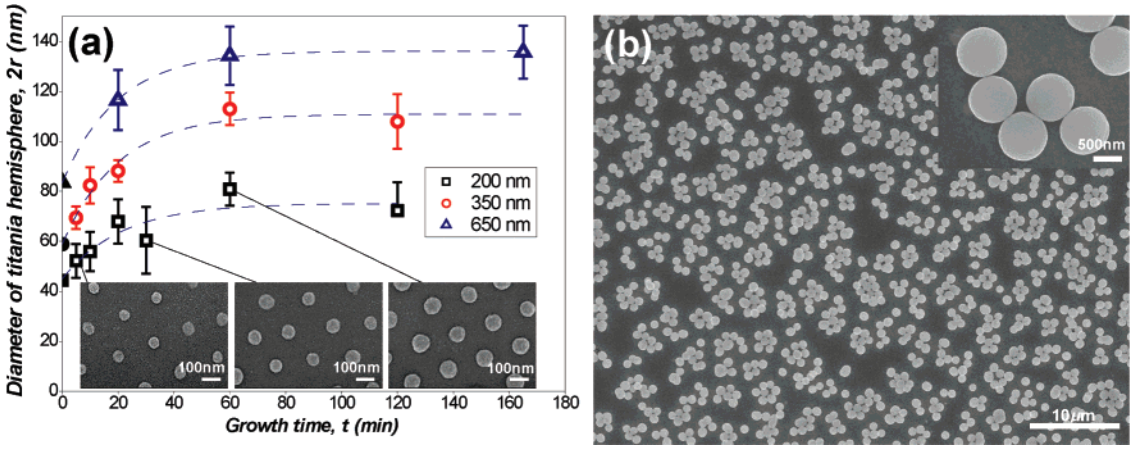

Figure 1. (a) Growth behavior of titania hemispheres on planar surfaces as a function of time. Oxide openings surrounded by OTS-SAMs with 200, 350, and 650 nm spacings were employed as nucleation sites. The open points are the experimental data; the dotted lines were applied for reasons of clarity. The initial sizes at $t = 0$, displayed with the close points, correspond to the dimension of the nucleation sites. For a time greater than approximately 60 min, the saturation of the growth comes from the exhaustion of the precursors in the solution. (b) Typical SEM image of colloidal particles harvested from the supernatant after the reaction finished. Average diameter: 1033 ± 83 nm.

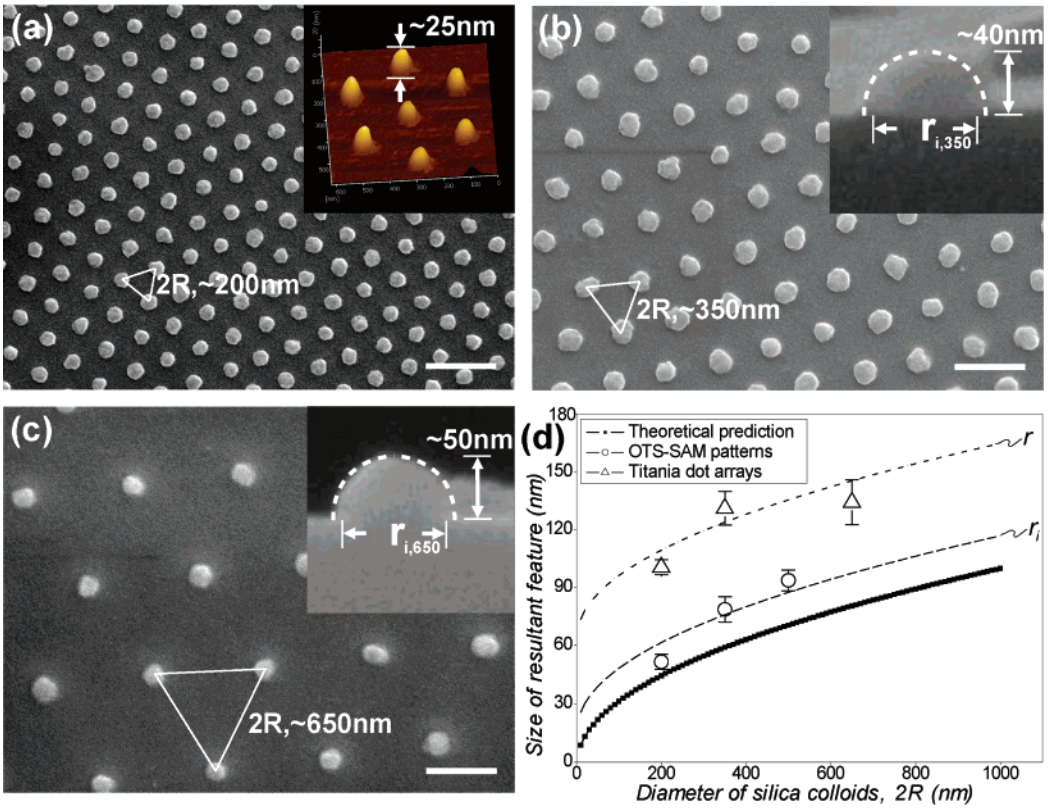

Figure 2. SEM of 2D arrays of titania hemispheres with (a) 200, (b) 350, and (c) 650 nm spacings; they were grown under identical growth conditions; all scale bars correspond to 400 nm. Insets: (a) AFM height image and (b, c) cross-sectional SEM images. (d) Experimental size of the resultant features as a function of the diameter of the silica colloids used: The solid squares represent a theoretical prediction of the size of the nucleation sites; the empty circles are the observed diameter of the oxide openings, which is also denoted as r_i; the empty triangles represent the experimental diameters of the titania hemispheres.

3. Results and Discussion

3.1. Site-Selective Titania Growth. Scheme 1 briefly illustrates the CAL concept used to prepare organic templates of SAMs at the nanometer scale for additionally growing materials on SiO_2/Si wafers. The growth of titania on silica surfaces was chosen as a model system for site-selective heterogeneous growth. The procedure for planar growth is described first, as shown in Scheme 1: (a) Fabrication began by convectively assembling monodisperse silica colloids ranging from 100 to 650 nm in diameter into a close-packed monolayer on a SiO_2/Si wafer.[13,14] UV−ozone treatments of ~1 h were conducted to further induce the hydroxyl group to the sample surfaces. (b) OTS-SAMs were then coated by immersing the sample in a toluene solution containing OTS molecules (typically 2.1 mM) for ~5 h. (c) The colloidal films serving as masks were detached by sonication in water. (d) Designated surfaces (i.e., oxide openings surrounded by OTS-SAMs) of the resulting chemical

(14) Bae, C.; Shin, H.; Moon, J. *Chem. Mater.* **2007**, *19*, 1531.

patterns served as nucleation sites for an additional growth of titania dots. The growth condition originally used by Jiang et al.[15] was adapted to obtain a uniform array of titania dots, except that the present experiments were carried out in ambient conditions.

Figure 1a shows the time evolution of the site-selective titania growth behavior starting from three different sizes of the opening (i.e., nucleation sites), ~44, 60, and 81 nm in diameter. After an instant injection of precursors into a solution containing a series of substrates with chemical patterns of different sizes, the radius of the resulting titania dots, r, was recorded as a function of time by determining it with atomic force microscopy (AFM) and field-emission scanning electron microscopy (FESEM). Although the contact area between an ideal sphere and a flat surface would be an arealess point, for CAL the contact area between two oxide surfaces has a dimension in that it introduces a thin organic layer (i.e., SAMs) onto the surfaces, approximating $A_{ox} = \pi(R^2 - |d - R|^2)$ where R represents the radius of the silica sphere and d is the thickness of the SAM layer. In addition to the geometrical consideration, the capillary condensation of liquid (e.g., water) at the contact menisci often leads to a small expansion (i.e., 5−10 nm) of the resulting pattern diameter.[13] Upon this careful treatment on the initial dimension of the nucleation sites, the growth characteristic curves were obtained from nucleation sites of three different sizes, as shown in Figure 1a. Each curve demonstrates saturation of the growth rate after ~1 h of immersion, indicative of the exhaustion of the precursor molecules in solution. This saturation characteristic hinders the understanding of the growth mechanism in detail. Nevertheless, the growth behavior before saturation suggests that the growth is controlled by diffusion. Below the saturation time, as shown in Figure 1a, the experimental data are well fit by an equation for the diffusion-controlled growth,[16] $r = \sqrt{k_D t + r_i^2}$, where r is the radius of the titania dots, k_D, a constant related to diffusion, and r_i, the radius of the nucleation sites. It is noted that the expected and observed dimension of the openings, r_i, using CAL, showed an excellent agreement with the fitted values with the equation at $t = 0$, as shown in Figure 1 (Black-filled triangle, circle, and square). At $t = 0$, instant heterogeneous nucleation and subsequent diffusion-controlled growth can be assumed for the site-selective growth of titania.

Additional evidence regarding the diffusivity of precursor molecules was also obtained by carrying out the same experiment under the enhanced flux velocity of the system such as ultrasound irradiation, resulting in much larger titania hemispheres (i.e., a higher growth rate; data not shown here). It is also worth noting that much bigger spherical particles (~1 μm) with a narrow size distribution were harvested from the supernatant after the reaction finished (Figure 1b). This large difference in the growth rate between the titania dot arrays in the chemical pattern surfaces and the titania particles grown in the solutions is a result of the difference between the concentration gradients of the precursor molecules at the diffusion field near the two types of growing materials. The growth rate v is proportional to the concentration gradient $\partial C/\partial z$.[17] Assuming

Scheme 2. Schematic Illustration of the Site-Selective Growth Process on Silica Colloidal Crystals[a]

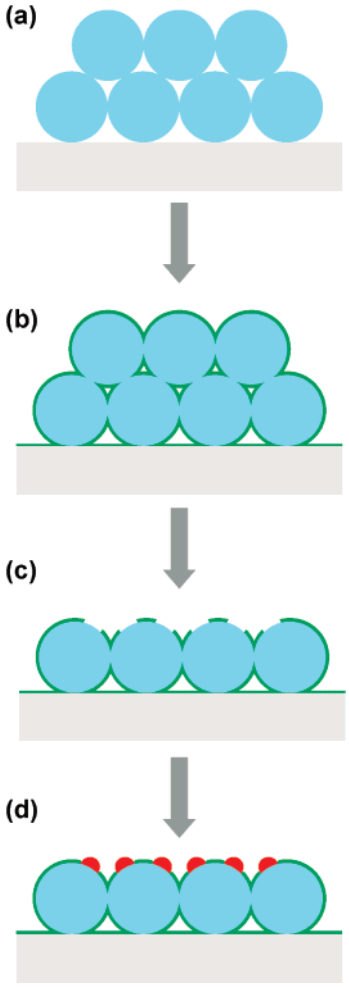

[a] (a) Silica colloidal crystals with several layer thick are formed on SiO_2 substrates through convective assembly. (b) OTS-SAMs are coated on the whole surfaces except for both the colloid−substrate contacts and the colloid−colloid contacts. (c) The upper layers of the SAM-coated colloids are detached with tape in order to open the oxide nucleation sites. (d) Asymmetric colloidal clusters are fabricated from the chemically nanopattered colloids by the site-specific nucleation and growth process.

the homogeneous bulk concentration in the system, the diffusion field length for the growth of the suspended spheres is reduced due to their Brownian movement in the convective bulk solution that results in a sharp concentration gradient and subsequent faster growth rate. In the biological world, it is also believed that specialized biomolecules control biomineralization by diffusion-controlled mechanisms.[18] Our results also show biological relevance in the low-temperature synthesis of ceramic materials in nature.[19]

The site-selective characteristic of the modified sol−gel reaction is further demonstrated by the morphological development. Figure 2a−c show a series of titania arrays with different spacings, demonstrating the superior controllability and reproducibility of this approach. The average diameters (spacings) of the hemispheres are 100.6 ± 3.9 (200), 131.2 ± 8.7 (350),

(15) Jiang, X.; Herricks, T.; Xia, Y. *Adv. Mater.* **2003**, *15*, 1205.
(16) Cao, G. *Nanostructures and nanomaterials: synthesis, properties, and application*; Imperial College Press: London, 2004.
(17) Saito, Y. *Statistical physics of crystal growth*; World Scientific: Singapore, 1996.
(18) Lowenstam, H. A.; Weiner, S. *On Biomineralization*; Oxford University Press: London, 1989.
(19) (a) Aizenberg, J.; Sundar, V. C.; Yablon, A. D.; Weaver, J. C.; Chen, G. *Proc. Natl. Acad. Sci. U.S.A.* **2004**, *101*, 3358. (b) Aizenberg, J.; Weaver, J. C.; Thanawala, M. S.; Sundar, V. C.; Morse, D. E.; Fratzl, P. *Science* **2005**, *309*, 275.

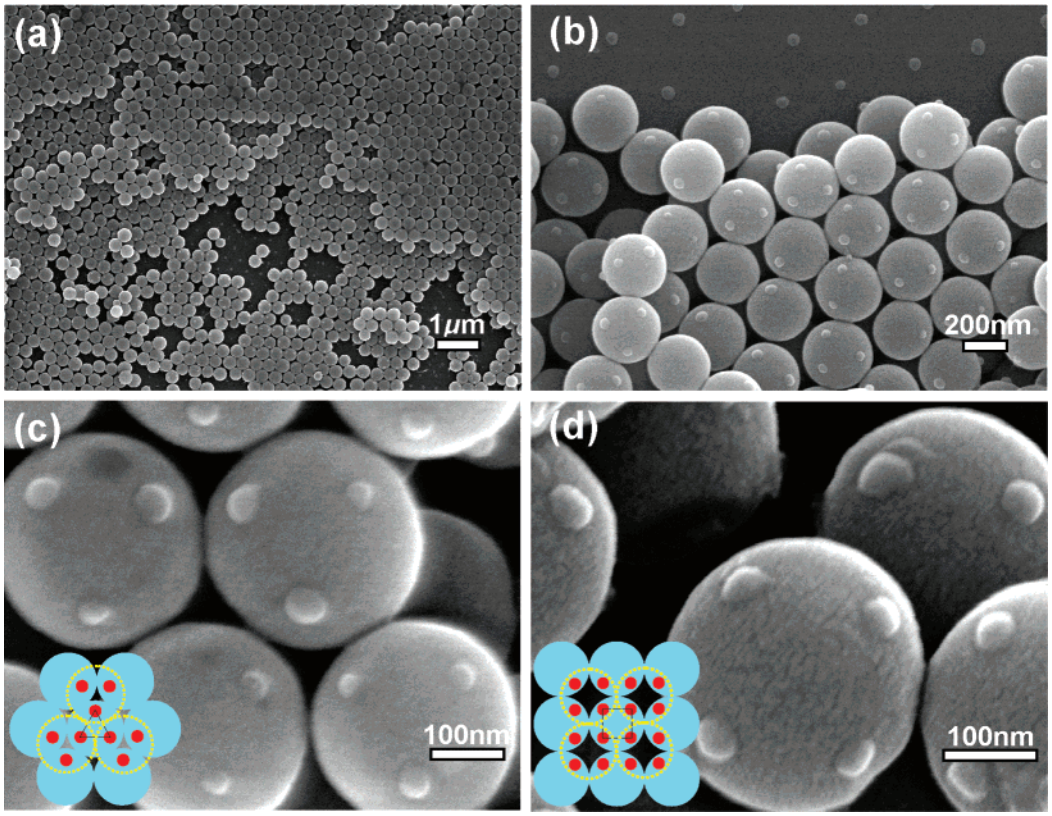

Figure 3. SEM micrographs of asymmetric colloidal clusters (ACCs) consisting of titania/silica. (a) An experimental result is shown as proof of concept; a monolayer of ACCs was prepared on a planer surface from the silica colloidal crystals with double layers in which the upper layers of silica were removed before the site-selective growth of titania. (b) ACCs in a certain region are more than two layers; the pieces having one or two titania dots are resulted from the insecure contacts with the upper silica layers. Panel (c) is from the (111) surface of the underlying colloidal films; panel (d) is from the (100) facet. The solid blue circles in the insets indicate the underlying silica colloids, and the dotted yellow lines indicate the upper layer detached to open the nucleation sites; the solid red circles represent titania dots selectively grown on the oxide openings of the silica spheres.

and 134.3 ± 11.7 (650) nm, respectively, as shown in Figure 2d (empty triangle). The growth evolution in the proposed system differs from typical heteroepitaxy growing with an equilibrium aspect ratio[20,21] in that the accomplishment of the modulation of the surface energy makes it possible to grow materials site-selectively with an extremely narrow size distribution. To be precise, it does not involve constant radial advancement of the growing interfaces where the methyl surfaces of the OTS-SAM templates act as surfaces with no binding sites as well as lower energy surfaces that determine the advancing direction of the three-phase contact line of the system. Due to the lower energy of the OTS-SAM surfaces compared to the nucleation sites of the silica,[13] equilibration of the surface tensions at the three-phase contact line in the growing materials leads to growth mostly within the area of the nucleation sites or radial growth with the suppression of the growth parallel to the substrate into the OTS surfaces. A relatively small advancement of the three-phase contact line ($r - r_i$, 20−30 nm) is clearly observed, while the growth height reaches 40−50 nm, as shown in the insets of Figure 2b and c, which is indicative of site specificity.

3.2. Fabrication of Asymmetric Titania/Silica Colloidal Clusters. It was also demonstrated that the strategy used for the site-selective growth on SiO_2/Si wafers can be applied to colloidal spheres in order to construct assembling objects with complex shape and especially ACCs (Scheme 2). Monodisperse silica colloids were first crystallized into a close packed structure several layers thick either on a silicon wafer or a glass microscope slide (a). UV−ozone treatments were conducted for the same purpose as that for the planar growth. The surfaces of the crystallized colloids were coated with OTS-SAMs, except for the areas touching the nearest-neighbors of the colloids, by immersing them in a 2.1 mM OTS solution (b). The substrate was then rinsed with chloroform to remove any excess OTS molecules that otherwise would be physisorbed upon the SAM-coated opal framework. After drying the solvent, the upper layers of the OTS-coated colloids were detached with tape to expose the OTS-patterned colloids (c). Additional dots of titania were deposited onto the exposed oxide openings of silica spheres with conditions identical to those for the planar growth (d).

In this case, according to the preferential orientation of the colloidal crystals consisting of silica spheres with respect to the substrate, the number and position of the resulting titania dots on the underlying sphere were determined. When the crystal orientation is (111) parallel to the substrate, each sphere has three contacts against the upper colloidal layer; thus, three additional dots with triangular geometry formed on each sphere (Figures 3c). Four additional dots with rectangular geometry on each sphere were also created from the (100) facets (Figures 3d). Such square arrays of spheres can be found in a colloidal crystal film grown on planar solid substrates, as in this case, although the [111] surfaces are dominant.[22] The average

(20) Johnson, H. T.; Freund, L. B. *J. Appl. Phys.* **1997**, *81*, 6081.
(21) Kamins, T. I.; Ohlberg, D. A. A.; Williams, R. S.; Zhang, W.; Chou, S. Y. *Appl. Phys. Lett.* **1999**, *74*, 1773.

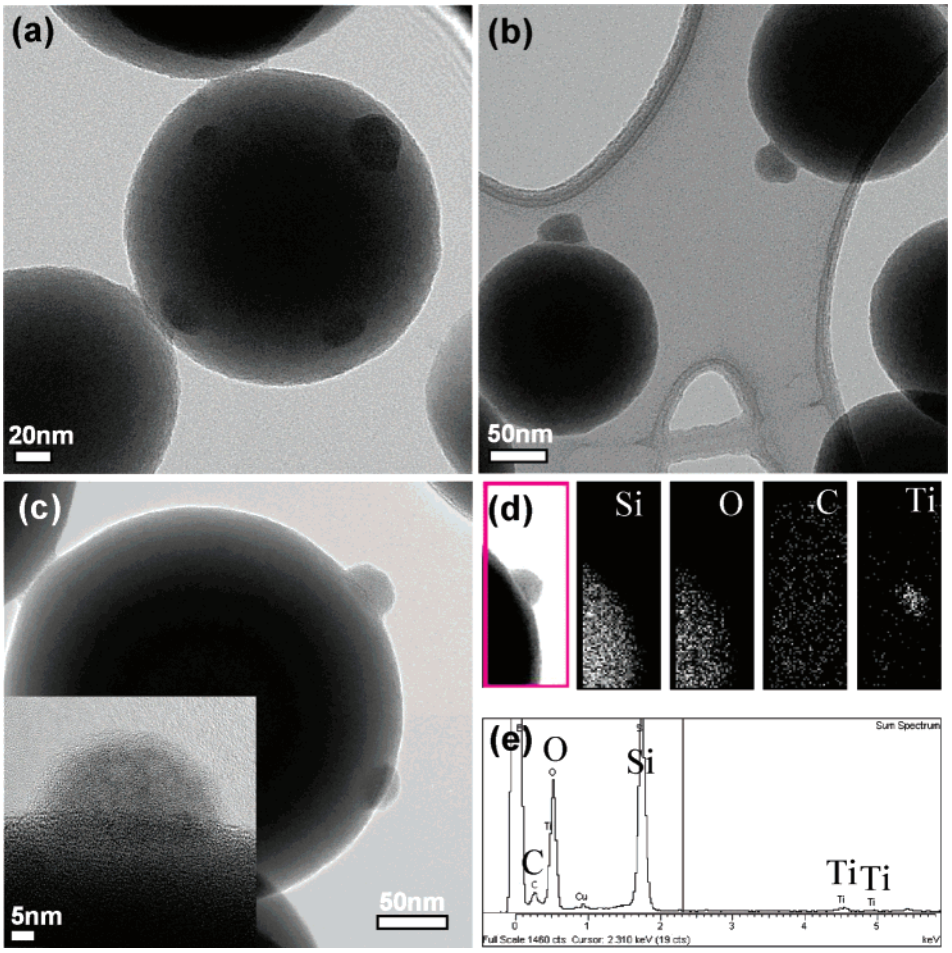

Figure 4. TEM micrographs and EDS analysis of titania/silica asymmetric colloidal clusters (ACCs). (a) An ACC with rectangular geometry whose curvature radius is about 50 nm and titania dots have a dimension less than 20 nm which are the smallest structures to date. (b) Some ACCs that show evidence of the site-selective growth; when the titania is grown in excess of the dimension of the initial nucleation sites, it grows with the equilibration in the surface energy, producing truncated spheres. (c) 530/30 nm ACCs whose magnified image shows that the selectively grown titania is hemispherical. (d) EDX maps of a part of ACCs taken in the magenta rectangular area (left image); the bright contrasts imply the presence of certain elements (from left to right: silicon, oxygen, carbon, and titanium, as depicted in the upper right part of each map). (e) A typical EDX spectrum of the titania/silica ACCs.

diameter of the dots is ~30 nm when silica spheres of 280 nm are used. The correlation between the radius of the oxide openings, $r_{i,c}$, and the radius of the underlying sphere obeys the following equation: $r_{i,c} = \sqrt{2R \cdot d + d^2}/2$. Assuming that $d = 2.5$ nm for the thickness of OTS-SAMs and $2R = 280$ nm, the resulting diameter, $2r_{i,c}$, of the opening is ~27 nm which is in excellent agreement with the value taken from the EM micrographs.

The success of the site-selective growth of titania was also confirmed with high-resolution transmission electron microscopy (HRTEM) and energy-dispersive X-ray spectrometry (EDS), as shown in Figure 4. The structure and composition of the as-deposited materials were identified as titanium-containing, carbon-rich amorphous oxide on the basis of electron diffraction (data not shown here) and EDS, as also confirmed by Jiang et al.[15] The titanium-containing amorphous materials can also be converted to anatase or rutile polymorphs through annealing.[15] However, with appropriate precursors[19] and nucleation site dimensions,[23] crystalline materials with controlled polymorphism may be directly deposited by this strategy.

3.3. Optical Properties of Asymmetric Colloidal Clusters. An essential issue involving the characterization and application of the ACCs relates to their optical properties associated with the photonic band gap. To study the optical properties of the resulting titania/silica ACCs, the optical absorption spectra were obtained (complementarily, transmission and reflection spectra were also recorded, but the same spectral positions were observed). The spectra taken before growing titania dots exhibit distinct two peak patterns in optical density for both samples of 466 and 650 nm silica colloids (black and green lines in Figure 5). For longer wavelengths, these spectral patterns come from the silica colloidal crystals that are several layers thick and correspond to the pseudogap between the second and third bands at the L point of the first Brillouin zone, as confirmed with the modified Bragg law,[7c] $\lambda_{max} = 2D\sqrt{\epsilon_{eff}}$ where D is the distance between the crystal planes and ϵ_{eff} is the volume-averaged effective dielectric constant; $\epsilon_{eff} = (n_1)^2 f + (n_2)^2(1 - f)$ where f is the crystal filling fraction and n is the refractive index. That is, the peaks at 1010 (black line in Figure 5) and 1380 nm (green line in Figure 5) in the near-infrared (NIR) region could be assigned to the positions of the (111) stop gaps of 466 and 650 nm silica ($n_1 = 1.425$) colloidal crystals,

(22) Velev, O. D.; Lenhoff, A. M.; Kaler, E. W. *Science* **2000**, *287*, 2240.

(23) (a) Ranade, M. R.; Navrotsky, A.; Zhang, H. Z.; Banfield, J. F.; Elder, S. H.; Zaban, A.; Borse, P. H.; Kulkarni, S. K.; Doran, G. S.; Whitfield, H. J. *Proc. Natl. Acad. Sci. U.S.A.* **2002**, *99*, 6476. (b) Navrotsky, A. *Proc. Natl. Acad. Sci. U.S.A.* **2004**, *101*, 12096.

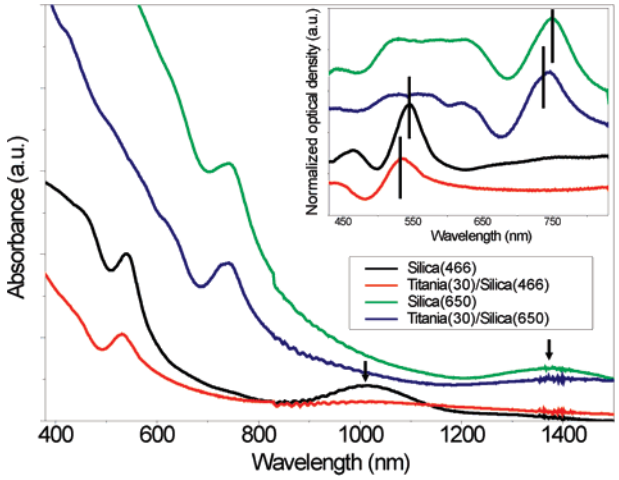

Figure 5. Normal-incident absorption spectra of different thin colloidal crystals: The green line was taken from a thin colloidal crystal made of 650 nm diameter silica, and the blue line was taken after the deposition of titania with the same crystal. The black line was taken from a thin colloidal crystal made of 466 nm diameter silica, and the red line was taken after the deposition of titania with the same crystal. The black arrows indicate the (111) stop gaps of the silica colloidal crystals. The inset shows the normalized optical intensity of the peaks in the visible region of both of the titania/silica ACC samples after extraction of the absorption intensity. The colors of each spectrum are identical to those in the full spectra; the strong fluctuation in this energy region is typical in colloidal photonic crystals. The spectra were vertically offset for reasons of clarity.

respectively. After detaching the upper layers of the silica colloids to open the nucleation sites, attenuation of the intensity of these peaks indicates that the thickness of the crystal films decreased (blue and red lines in Figure 5). As a result of the attenuation, we could not observe any spectral shifts in this energy region after growing the dots.

For the spectral feature of colloidal photonic crystals being observed at the high-energy region, their exact origin is not fully understood and is still under debate. Several possible explanations have been proposed by other researchers, including [220] Bragg diffraction,[24] high reflectivity from the low band-dispersity,[25] and whispering gallery mode (WGM).[26] First, for the [220] Bragg diffraction, Míguez and his co-workers have recently shown that the high-energy spectral patterns cannot be associated with the absence of photon states by calculating colloidal photonic band structures in detail.[25] It is also worth pointing out that the peaks do not result from absorption by any materials, by demonstrating that the peak positions shift by the change in the periodicity of colloidal films. A second possible explanation is the effect on increased effective refractivity at the higher Brillouin zones' boundaries,[25] which is consistent with the notion demonstrated in 2D photonic crystals experiments.[27] In addition to this approach on the basis of multiple scattering, third, resonance theory based on a single scatterer also provides a similar result for optical spectroscopic patterns of photonic crystals.[28] Guo et al. have observed the strong fluctuation in optical spectra of thin colloidal photonic

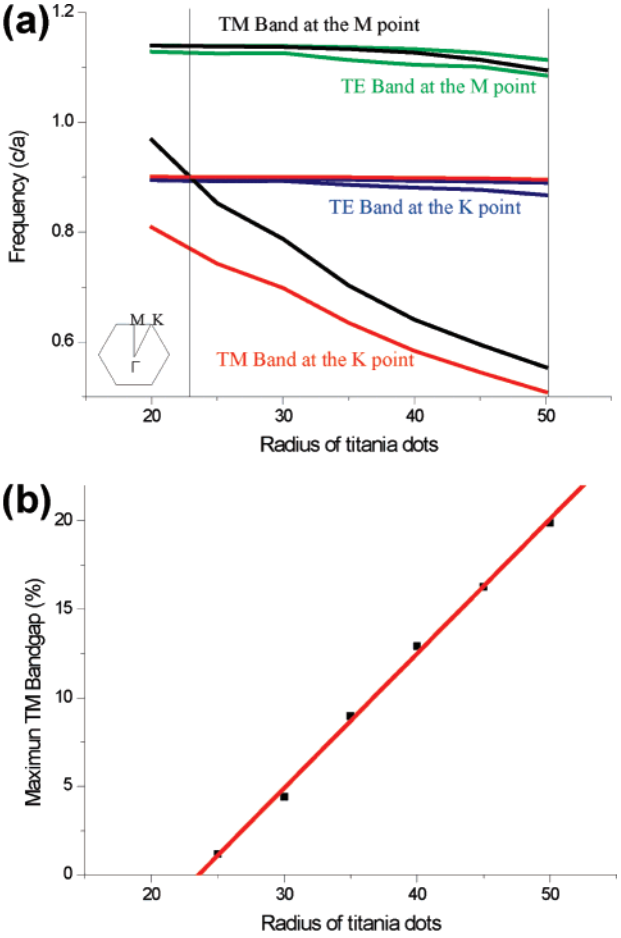

Figure 6. Photonic band calculation of triangular titania arrays in two-dimension format with 200 nm interdot spacing as a model system as a function of the filling fraction. Principal directions in k space are illustrated in the inset of (a). The first and second bands in the two principal directions were plotted as a function of the filling fraction. Lower bands are the first bands, and upper bands are the second band for each color. Calculation results show that the TE bands between the M and K points exhibit no overlap for any filling fractions. However there exists a marked overlap between the first TM band at the M point and the second TM band at the K point when the dot diameter is larger than ~50 nm, indicating that a photonic band gap opens for the TM polarization. (b) The maximum TM gap as a function of the filling fraction.

crystal film made of three layers of latex spheres and proposed that such a feature is originated from the propagation of the WGM. When a single sphere excited by resonance conditions inside itself is placed close to another sphere, the confined waves can propagate toward another particle. The resonance can enhance when the waves pass along regularly arrayed colloidal particles, obeying $2\pi R = m\lambda/n$ ($m = 1, 2, 3,...$), where λ is the wavelength of light and the other symbols are the same as those previously. By adopting this optical mode, we found that the central wavelengths of the maximum peaks (748 nm for green line and 545 nm for black line) at the high-energy region can be assigned to the resonant peaks of 727 and 521 nm, respectively, where $m = 4$. Small differences between experimental and calculated values can be explained by the change of effective optical index in such a high-energy region.[29]

After growing titania hemispheres on the hydroxyl openings of the underlying silica spheres, a little blue shift of ~10 nm at

(24) (a) Míguez, H.; López, C.; Meseguer, F.; Blanco, A.; Vázquez, L.; Mayoral, R.; Ocaña, M.; Fornés, V.; Mifsud, A. *Appl. Phys. Lett.* **1997**, *71*, 1148. (b) Jeong, U.; Xia, Y. *Adv. Mater.* **2005**, *17*, 102. (c) Jeong, U.; Xia, Y. *Angew. Chem., Int. Ed.* **2005**, *44*, 3099.
(25) Míguez, H.; Kitaev, V.; Ozin, G. A. *Appl. Phys. Lett.* **2004**, *84*, 1239.
(26) Guo, H.; Chen, H.; Ni, P.; Zhang, Q.; Cheng, B.; Zhang, D. *Appl. Phys. Lett.* **2003**, *82*, 373.
(27) (a) Rosenberg, A.; Tonucci, R. J.; Lin, H.-B.; Shirley, E. L. *Phys. Rev. B* **1996**, *54*, R5195. (b) Rosenberg, A.; Tonucci, R. J.; Bolden, E. A. *Appl. Phys. Lett.* **1996**, *69*, 2638.
(28) Lidorikis, E.; Sigalas, M. M.; Economou, E. N.; Soukoulis, C. M. *Phys. Rev. B* **2000**, *61*, 13458.
(29) Furukawa, H.; Tenjimbayashi, K. *Appl. Phys. Lett.* **2002**, *80*, 192.

the peak was observed at the high-energy region for both samples as shown in the inset of Figure 5. The similar blue shifts were also detected in the sample in different regions. We thought of various possible causes of this blue shift in order to clarify its origin. First, it is noted that the case of infiltration of materials with higher[30] or the same[31] refractive index into photonic crystal films made of monodisperse silica spheres, in general, results in red-shifts. Therefore undesired deposition of titania in the underlying opal film is not a possible source of the blue shift. To verify whether this shift is from the ordered 2D arrays of dielectric hemispheres, photonic bands of the 2D crystals were calculated[32] in two principal directions for both polarizations as a function of the filling fraction of the dots (Figure 6). The results show that the titania arrays only have a photonic band gap for only TM-polarized light, and thus this spectral blue shift could not have resulted from the periodicity of the titania dots sitting on the selective nucleation sites. Finally, we considered that if the fluctuation behavior at the shorter wavelength region was caused by the WGM, the little blue shift would be a result of a decreased volume averaged refractive index of the present system consisting of titania/silica ACCs. Although the material of higher optical index ($n_3 = 1.88$, ref 15) was deposited onto the silica ($n_1 = 1.425$) spheres, the volume averaged indexes of the modified spheres (i.e., titania/silica particles) were slightly decreased from 1.425 for pure silica to 1.378 for 30/466 particles and 1.393 for 30/650 particles. In this case, however, the effective volume of the modified spherical cavity is also increased and is more dominant to the resonant frequency than the decreased refractive index. Indeed all of the effective radii of the present systems from R to $R + r_{i,c}$ were investigated, but the calculated values indicated that the central position of the resonant peaks should be shifted to a longer wavelength. In accordance with the observation by Furukawa and Tenjimbayashi,[29] finally, some of the propagating light leaks at the contacts between spheres in the colloidal film. These leakages can induce the intensity reduction of the spectrum as well as a small spectral shift, so we think that the blue shift in the optical spectra of the present systems may be explained by the added leakage paths after the deposition of titania dots since the dots are formed at the contact points between the original silica spheres.

(30) (a) King, J. S.; Graugnard, E.; Summers, C. J. *Adv. Mater*. **2005**, *17*, 1010. (b) King, J. S.; Gaillot, D. P.; Graugnard, E.; Summers, C. J. *Adv. Mater*. **2006**, *18*, 1063.
(31) Míguez, H.; Tétreault, N.; Hatton, B.; Yang, S. M.; Perovic, D.; Ozin, G. A. *Chem. Commun.* **2002**, 2736.
(32) MIT Photonic-Bands, package, Johnson, S. G.; Joannopoulos, J. D. *Opt. Express* **2001**, *8*, 173.

4. Conclusion

Here we report an example of site-specific heterogeneous nucleation and growth of materials at the sub-100 nm length scale. Our results show that the nanometric site-specificity can be accomplished by a combination of the diffusion-controlled mechanism and the large difference of surface energy between the growing and the surrounding surfaces. It is also shown that site-specific modifications can be applied to the curved surfaces (curvature radius less than 100 nm) of individual small objects such as colloidal spheres, producing complex, multifunctional building blocks (i.e., ACCs) that would be difficult or impossible to create by any other lithographic methods. Furthermore, the optical properties of the thin layers consisting of ACCs were investigated in terms of the photonic band gap. The bottom-up approach reported here could serve as a promising route for fabricating nanoscale arrays for a variety of materials as well as for patterning highly curved surfaces leading to the creation of assembling small objects with a high degree of shape complexity.

Acknowledgment. The authors thank Pil-Ryung Cha for his helpful comments and discussion. This work was supported by the Nano R&D Program (M10503000255-05M0300-25510, 2005-02522) of the Korean Ministry of Science and Technology (MOST), by the Center for Materials and Processes of Self-Assembly (R11-2005-048-00000-0) under the ERC/SRC programs of MOST/the Korean Science and Engineering Foundation (KOSEF), and by the Center for Nanostructured Materials Technology (M105KO010026-06K1501-02610) under the 21st Century frontier R&D Programs of MOST. C.B. was partially supported by the Seoul Science Fellowship Program of Seoul City, Korea.

JA073043P